DiffuSyn Bench: Evaluating Vision-Language Models on Real-World Complexities with Diffusion-Generated Synthetic Benchmarks

Haokun Zhou[1★][0009−0001−5955−285X] and Yipeng Hong[2★][0009−0000−9896−5617]

[1] University of Nottingham, Ningbo, China
hnyhz13@nottingham.edu.cn
[2] Shanghai Maritime University, Shanghai, China
hongyipeng@stu.shmtu.edu.cn

Abstract. This study assesses the ability of Large Vision-Language Models (LVLMs) to differentiate between AI-generated and human-generated images. It introduces a new automated benchmark construction method for this evaluation. The experiment compared common LVLMs with human participants using a mixed dataset of AI and human-created images. Results showed that LVLMs could distinguish between the image types to some extent but exhibited a rightward bias, and perform significantly worse compared to humans. To build on these findings, we developed an automated benchmark construction process using AI. This process involved topic retrieval, narrative script generation, error embedding, and image generation, creating a diverse set of text-image pairs with intentional errors. We validated our method through constructing two caparable benchmarks. This study highlights the strengths and weaknesses of LVLMs in real-world understanding and advances benchmark construction techniques, providing a scalable and automatic approach for AI model evaluation.

Keywords: Vision language model · Benchmark · Synthetic data · Latent diffusion model

1 Introduction

In recent years, remarkable advances in deep learning within the fields of computer vision and natural language processing have propelled Large Vision-Language Models (LVLMs) to the forefront as powerful tools for understanding and interpreting visual and textual data. Despite their impressive capabilities, the extent to which these models can accurately comprehend and analyze real-world scenarios remains a subject of ongoing investigation. This essay embarks on a dual-fold exploration: firstly, it assesses the capacity of LVLMs to differentiate between AI-generated and human-originated images—a task that probes their ability to interpret and understand nuanced visual information. Secondly, it extends these

---

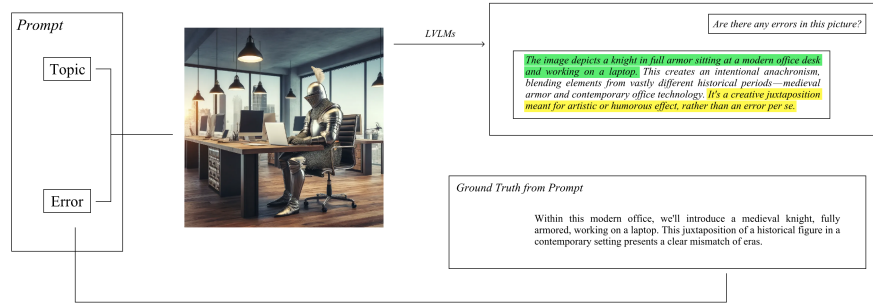★ These authors contributed equally to this work.

Fig. 1. This is a simple example that shows a brief framework for benchmark generation process and provides a specific example from our benchmark, showcasing the response from GPT-4V to our tests. The example image features a modern office setting with a medieval knight working on a laptop, highlighting the intentional anachronism. This example also reveals why GPT-4V may have underperformed in the initial part of our test, potentially due to alignment issues.

insights to the systematic development of a methodology for the automatic generation of benchmarks designed to evaluate this ability.

The first part of our study focuses on a rigorous examination of LVLMs' performance in identifying anomalies and errors within images, utilizing a dataset comprising both AI-generated and human-created visuals. This evaluation is critical for understanding the models' proficiency in real-world understanding, as well as their ability to discern subtle differences in image quality and content.

Building upon these findings, the second part of the essay delves into the development of an automatic benchmark construction methodology. This innovative approach involves the use of AI techniques to generate and validate benchmarks, providing a scalable and efficient means of testing LVLMs' capabilities. By integrating automated processes, we aim to create robust and reliable benchmarks that can be utilized to continuously assess and improve the performance of LVLMs in various real-world tasks.

Through a combination of experimental evaluation and methodological innovation, this essay provides a comprehensive overview of LVLMs' abilities and the potential for AI-driven benchmark construction. Our findings contribute to the broader understanding of LVLMs' real-world comprehension and pave the way for future advancements in AI model evaluation and development.

2   Recognizing LVLMs' ability to understand the real world

Recently, generative models have made significant strides in synthesizing realistic images. Various text-to-image generative models, exemplified by Latent

Diffusion Models (LDM), have blurred the lines between computer-generated and real-world images. Prominent models such as Midjourney[3], DALL-E[1], and Stable Diffusion[2], built on denoising autoencoders, exhibit an exceptional ability to produce lifelike images. Concurrently, discriminative methods rooted in traditional computer vision classification techniques, such as the CNN-based ResNet[4], transformer-based DeiT-S[5], and Swin-T[6], have been explored for their effectiveness in distinguishing text-to-image (T2I) creations in the existing literature[7]. Despite these advances, a critical observation in this domain is the inherent limitation of these models in replicating the fidelity of the real world. Unlike algorithm-based feature extraction, humans possess an innate ability to discern AI-generated images by identifying intrinsic errors or anomalies.

This observation has propelled our investigation into the capabilities of Large Vision-Language Models (LVLMs), which have demonstrated impressive performance across various tasks and exhibit human-like responses to images by integrating visual and textual processing abilities.

3   Method

3.1   Overview

This experiment aims to evaluate the ability of Large Vision Language Models (LVLMs) to distinguish between AI-generated and human-generated images and to compare their performance with that of human participants. We utilize GPT-3.5 to process the LVLMs' responses into binary data for analysis.

3.2   Image Dataset

The dataset includes 2000 images, evenly split between AI-generated images and those created by human artists. The AI-generated images include blends generated by several renowned diffusion models, including Stable Diffusion 2.1, Stable Diffusion 1.5, and DALL-E 3. The Stable Diffusion images are sourced from Poloclub's DiffusionDB dataset, while the DALL-E 3 images are selected from LAION's DALL-E 3 dataset. The human-generated images are sourced from diverse and publicly available collections, selected to cover a wide range of subjects and styles. All images are standardized to a resolution of 512x512 pixels to ensure uniformity.

3.3   Experiment Settings

For GPT-4V, we utilized the API endpoint specifically designated for the GPT-4-1106-Vision-Preview, dated November 6, 2023. For the other models, we employed a selection of publicly accessible models and corresponding endpoints, conducting the experiments using a computational setup consisting of two blocks of A100 cloud servers.

The methodology involved a meticulous process of prompt selection. Various prompts were iteratively tested to ascertain their effectiveness in two key areas:

categorizing images using LVLMs and directing human participants to perform the same task. For example, initial prompts that directly asked if an image was AI-generated often led to refusals or biased answers, whereas descriptive prompts about image quality yielded better results. The specific prompts finalized for the experiment are detailed in the appendix of this document.

A critical parameter in our experimental design was the 'temperature' setting, which was fixed at 0. This decision was driven by the necessity to minimize variation in the model's output, ensuring a more deterministic and stable output, crucial for the reliability of the categorization process.

3.4   Procedure for LVLMs

The LVLMs were presented with each image in the dataset and tasked with identifying any anomalies or errors indicative of AI generation. Directly asking if the image is AI-generated or contains errors may result in a refusal to answer or affect the result due to the alignment of the LVLM. Therefore, following their analysis, the LVLMs provided a descriptive response for each image. The responses from the LVLMs were then processed through GPT-3.5-Turbo-1106, which was used to interpret the LVLMs' descriptive answers and convert them into binary outcomes: 'AI-generated' or 'Human-generated.' This conversion involves identifying specific patterns and keywords indicative of AI generation. This step standardizes the results for statistical comparison.

3.5   Procedure for Human Participants

Each human participant was presented with a randomized set of 200 images from the dataset, consisting of 100 AI-generated images and 100 images from human artists. They were instructed to categorize each image as either AI-generated or human-generated, relying on their judgment and observation. Human subjects were provided with the same prompt as the LVLMs, with no examples included and no time constraints imposed, allowing for careful consideration. Before the main task, participants underwent a brief training session (5 shots) with a different set of images to familiarize them with the task. The experiment did not include any subjects with knowledge related to NLP or CV, nor past experience in using diffusion models.

3.6   Statistical Analysis

The performance of LVLMs and human participants will be compared using statistical tests to evaluate the significance of their performance differences.

4   Result and Analysis

4.1   Overview of Findings

Our study's findings are delineated through two analytical representations: a confusion matrix and a bar chart. These visual aids serve to elucidate the dis-

cernment capabilities of Large Vision-Language Models (LVLMs) versus human participants in classifying images as either AI-generated or human-originated.

4.2 Observation and analysis

The construction of a confusion matrix forms the cornerstone of our analysis, partitioned into True Positives (TP), False Positives (FP), True Negatives (TN), and False Negatives (FN). In this framework, TP represents correct identifications of AI-generated images, while TN signifies accurate classifications of human-generated images. Conversely, FP and FN denote erroneous classifications. This structured approach enables a detailed examination of error patterns within both LVLMs and human cohorts.

Our findings highlight a notable inclination among LVLMs to misclassify images as human-generated, indicating a rightward bias. This tendency suggests a deficiency in LVLMs' comprehension of real-world textures and physical attributes, posing challenges in discerning subtle nuances characteristic of AI-generated imagery. However, we propose that this bias may be partly attributable to systemic alignment biases. Further analysis reveals instances where humans misclassify photographs lacking discernible AI-generated features as AI images, leading to an elevated FN rate. Conversely, examination of raw data unveils a predisposition in LVLMs, particularly GPT-4V, to reject AI-origin attributions even in the presence of detectable AI-specific features or when such features are erroneously identified. This disparity underscores the existence of systemic alignment biases in LVLMs, potentially impeding accuracy in positive identifications. (see Fig. 2)

4.3 Quantitative Analysis

In subsequent quantitative analyses, we employ accuracy and F1-score metrics to evaluate prediction efficacy. Accuracy gauges the proportion of correctly predicted instances relative to total predictions, while the F1-score, encompassing precision and recall, offers a nuanced performance assessment. Precision measures the ratio of true positive predictions to all positive predictions, whereas recall quantifies true positive predictions relative to all actual positive instances. Formally, the F1-score is defined as follows:

$$\text{F1-score} = 2 \times \frac{\text{TP}}{2 \times \text{TP} + \text{FP} + \text{FN}} \tag{1}$$

Human observers achieved an exceptional 88.45% accuracy in differentiating between AI and non-AI generated images, and have a similar correctness in both tasks. In contrast, all language-based AI models (LVLMs) produced lower overall correct rates, with the highest performing Fuyu-8B model achieving only 66.1% correctness and the lowest ranking LLaVA-1.5-13B model with a mere 50.5% correctness. As for the F1-score, Cogvlm, Qwen, LLaVA, Fuyu, and GPT-4V were 48.9%, 18.1%, 3.7%, 64.9%, and 28.0%, respectively, which was also
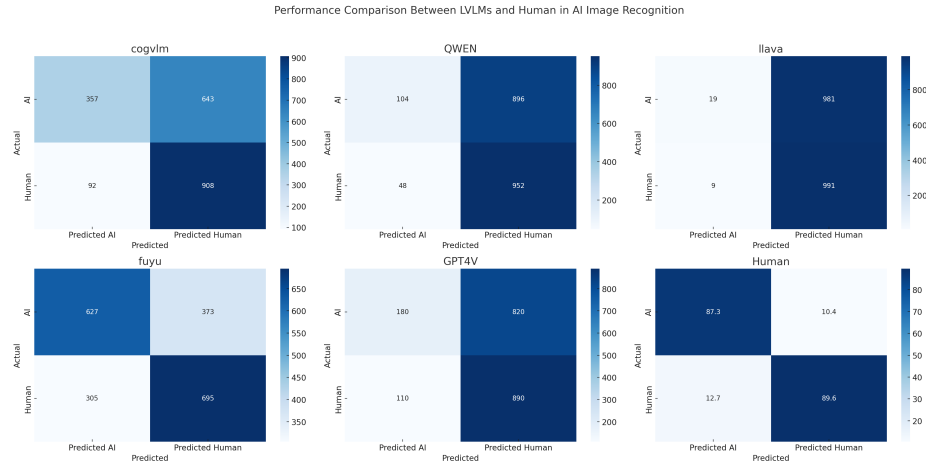
Fig. 2. showcases the performance comparison between different Large Language Models (LLMs) and humans in the task of distinguishing between AI-generated and human-generated images. The data is presented in six heatmaps, each representing the performance of one LLM or human. The x-axis in each heatmap denotes the predicted label (either "Guessed AI" or "Guessed Human"), while the y-axis denotes the actual label (either "Actual AI" or "Actual Human")..

significantly different from the 88.1% obtained by humans. From the results, the LVLMs show inefficient ability at the task of correctly recognizing AI-generated images and demonstrate a significant difference from human ability.

Chi-square tests for independence corroborate LVLMs' capacity to identify AI-generated content beyond chance, except for the LLaVA-1.5-13B model. This statistical significance underscores LVLMs' innate ability to detect errors indicative of AI-generated images, notwithstanding their inherent limitations.(see Fig. 3)

5   Automatic Benchmark Construction and Evaluation Based on Our Findings

Expanding upon our thorough examination of LVLMs' proficiency in real-world understanding, it is essential to situate our discoveries within the broader context of benchmark evaluations and to embark on the creation of a novel benchmark tailored to our investigative task. Our findings bear particular significance as the evaluation inherently revolves around AI image generation, suggesting that benchmark construction for this task could conceivably rely entirely on AI methodologies. Numerous benchmarks have previously focused on testing LVLMs' abilities across a wide range of areas, including MM-Vet[8], HallusionBench[9], humor understanding benchmarks[10], and MMMU[11]. Ad-
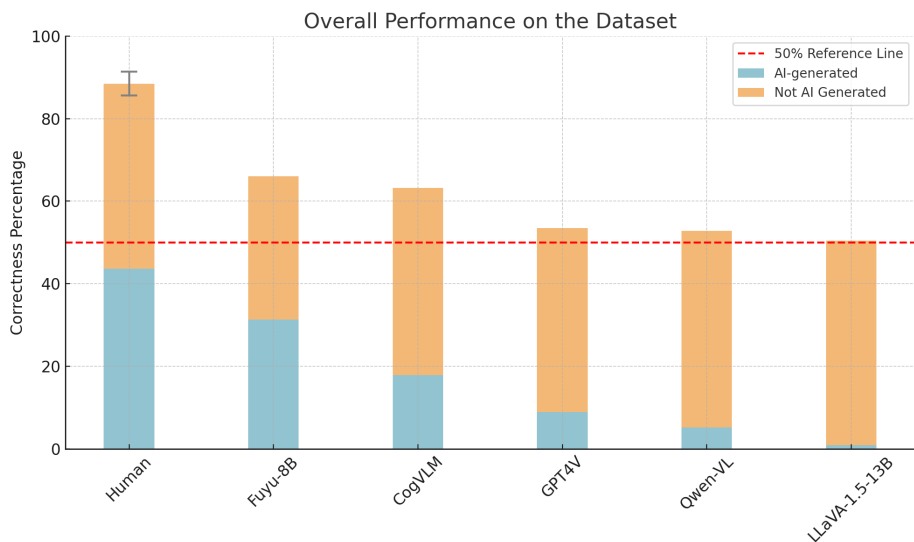
Fig. 3. compares the overall performance of humans and various models in identifying AI-generated and non-AI-generated images. The y-axis shows correctness percentages, while the x-axis lists the participants. The bars are divided into segments: blue for correctly identified AI-generated images and orange for correctly identified non-AI-generated images. The red dashed line at 50% marks the threshold for random guessing.

ditionally, benchmarks such as VisIT-Bench[12] and VASR[13] have concentrated on visual reasoning and real-world comprehension.

In light of these precedents, we now endeavor to craft an innovative benchmark framework that assesses LVLMs' aptitude in discerning AI-generated images and their ability to understand real-world contexts. Our observations suggest that a synthetic benchmark, constructed through a fully automated process, could be employed. This approach diverges from prior work, such as the use of Photorealistic Unreal Graphics (PUG)[16] to construct complex scenes. Instead, we propose leveraging AI-based methods to create benchmarks with broader capabilities, thereby enhancing the robustness and relevance of our evaluations.(see Fig. 4)

6   Method

Current text-to-image models often face many limitations, such as the lack of precise output control and 'illusions' that can cause their generated images to contain parts that are difficult to predict[14]. Additionally, they have difficulty combining multiple concepts, which leads to mixing items with different properties[15]. These problems can lead to unintended, problematic images. To minimize these issues, we devised a unique procedure to generate a dataset com-
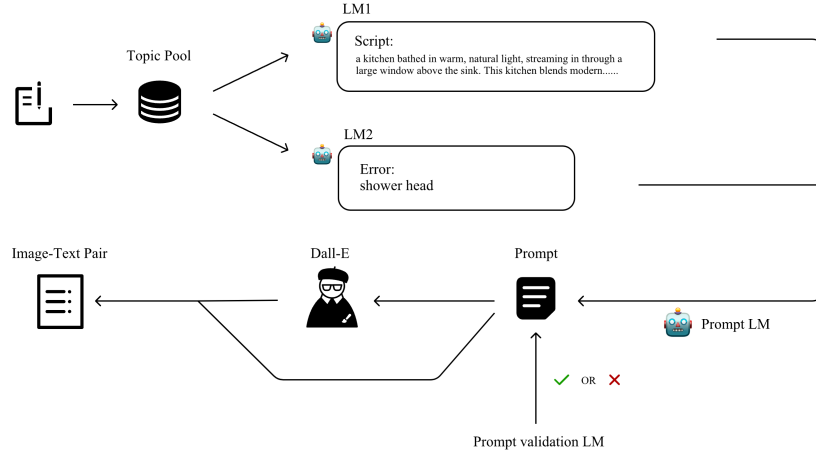
Fig. 4. An automated bench-marking framework designed to assess the proficiency of Large Vision-Language Models in identifying AI-generated images and understanding real-world contexts.

prising prompts with embedded errors and their visual representations. The process unfolds in several distinct stages, splitting the assignment of tasks to four language models and a text-to-image conversion model. Through this approach, we aim to challenge and assess the capabilities of LVLM models in recognizing and interpreting errors with a scalable and automatic method.

Topic Retrieval: The topic pool is a set of phrase entries which served as the topics of the text-image pair. Initially, a program randomly selects a phrase from the predefined topic pool and the same topic will be passed to both LM1 and LM2.

Narrative Script Generation: Utilizing GPT-4, we generate a detailed narrative script based on the retrieved topic. This script is designed to be comprehensive and contextually rich, setting the stage for the introduction of errors.

Error Generation: Parallelly, another instance of GPT-4 is tasked with generating a specific error related to the same topic. This error is intended to introduce a deliberate flaw or inconsistency within the context of the narrative script.

Prompt Synthesis with Embedded Error: Both the detailed narrative script and the generated error are then combined by a third instance of GPT-4. This step synthesizes a cohesive prompt that seamlessly integrates the narrative context with the specified error.

Evaluation of Prompt: Due to the limited capabilities of the text-to-image model, we found that in many cases, images do not efficiently perform

the prompts generated by the language model, e.g., 'the shadow of the tree faces the sun', which introduces noise to the dataset. We use a language model to act as a judge, controlling the type of error and the proportion of the image accounted for by the error, in order to increase the success rate of image generation.

Image Generation: The synthesized prompt, now containing the embedded error, is passed to DALL-E. Leveraging its text-to-image capabilities, DALL-E generates an image that visually manifests the embedded error, creating a direct visual representation of the narrative and error combination.

Benchmark Creation and Evaluation: Each text-image pair produced through this process establishes a unique benchmark within our dataset. To automate the evaluation of the model's ability to recognize and interpret errors in images, we use GPT-4, which compares pre-generated prompts to the model's responses, with individual scores ranging from 0 to 10, to quantify the accuracy of the model's responses.

The errors introduced into our benchmarks were systematically categorized into three distinct types:

- **Biological Errors**: These include anatomical anomalies, such as living beings missing essential parts or possessing extraneous ones, and behaviors that defy natural instincts or capabilities, exemplified by a fish capable of flight or a human engaging in photosynthesis.
- **Mismatched Eras**: This category captures errors involving anachronisms or the juxtaposition of elements from disparate historical periods without logical coherence, creating scenarios that challenge temporal understanding.
- **Logical Inconsistencies**: Encompassing functionality flaws—such as a door that leads to an impossible space—and incongruous object combinations that defy logical grouping or use, this category tests the model's ability to recognize and rationalize physical and conceptual discrepancies.

Upon generating and meticulously reviewing potential benchmarks, we dropped the noise and result a final set comprising 287, 289, and 272 text-and-image pairs for each error category, respectively. Through this framework, generation failures accounted for only 5.8% of all generated images, compared to 28.1% in the dataset where our generation architecture was not introduced, where prompts were generated by a single GPT4 and images were generated by the Dall-E 3 model. At the same time, the bias of the benchmark is also effectively controlled. When using a single LM, the three scenarios of kitchen, living room, and office occupy more than 90% of the total dataset, and even with higher temperature parameters, there are a lot of repetitive themes such as the error of introducing traffic lights in the kitchen, whereas after the introduction of our method, each of these scenarios accounts for no more than 5%.

7   Benchmark Result

We tested four LVLM models—CogVLM, GPT-4V, LLaVA, and Qwen—on our benchmark. The models were tasked with describing the errors present in the

images, and their outputs were compared to the error descriptions in the dataset, scoring them on a scale of 0-10 via GPT-4. From our results, GPT-4V demonstrated superiority in all three aspects compared to the other models. Specifically, we find that GPT-4V consistently outperforms comparable models in three categories: temporal error, biological error, and logical error.

Temporal Errors: Figure 3 shows the test results of the different models. GPT-4V scored a total of 2031 points for temporal errors, while its closest competitor, LLaVA, scored a total of 1347 points, indicating a large performance gap between the two.

Biological Errors: In terms of biological errors, GPT-4V earned a total score of 1268 compared to 796 for LLaVA and 657 for Qwen. This advantage suggests that GPT-4V may have a deeper understanding of images as well as the real world, enabling it to generate more accurate descriptions of image errors.

Logical Errors: Similarly, in terms of logical errors, GPT-4V's total score of 177 exceeds LLaVA's 164 and Qwen's 121. This also validates our observation in the previous section that GPT-4V's lower scores on the pairwise error discrimination task are mainly due to its stronger alignment, which leads to a refusal to recognize the presence of definite errors in the image.

Overall, the data show that GPT-4V consistently performs better across all error categories, confirming its superior capability in error recognition and description. However, the performance of all models on data other than temporal errors is poorer, which illustrates the fact that current LVLMs still have major limitations in terms of the consistency of image details with reality.(see Fig. 5)
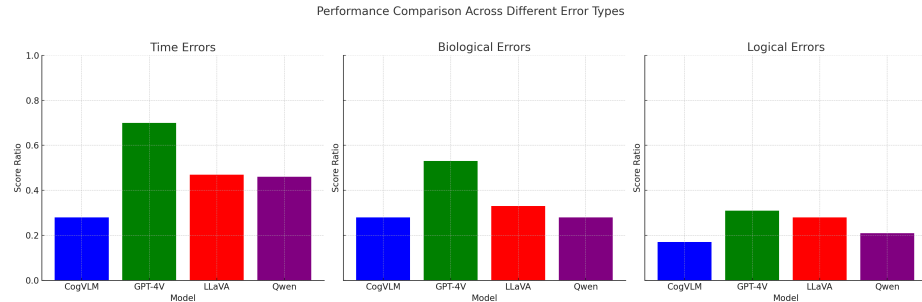

Fig. 5. The performance of four models across three types of errors, GPT4V achieve outstanding scores among three aspects.

To further validate our benchmark generation method, we conducted additional experimental evaluations. We created two other comparable benchmarks using different methodologies. In one benchmark, we selected images with obvious errors from a public diffusion model dataset and manually described the errors. In the other, we used human-authored prompts containing errors and employed the same image generation model to complete the dataset. We then tested the same LVLMs on these new benchmarks and recorded their scores.

We tested the same LVLMs on these new benchmarks and recorded their scores, as shown in Fig. 6. Comparing the original dataset with the human-authored prompts benchmark, we observed no significant differences in LVLM scores. However, in the comparison with the manually screened and labeled dataset, we found that the scores of all the LVLMs were reduced, and upon observation of the dataset, this was due to the limited control that Dall-E 3 has over the generated images. Errors in images from public datasets often stem from the diffusion model's inherent limitations rather than the specified input prompt, resulting in less obvious errors and smaller error areas. Despite these differences, the ranking of LVLMs' abilities remained consistent, with a Spearman rank correlation of 0.93 (p < 0.001) between our synthetic benchmark and the manually labeled benchmark. This consistency underscores the validity of our benchmark in assessing LVLMs, despite the synthetic dataset being less challenging.This shows our benchmark maintains relatively great assessment validity while using automated synthesis methods, and can effectively evaluating the real-world capabilities of LVLMs.
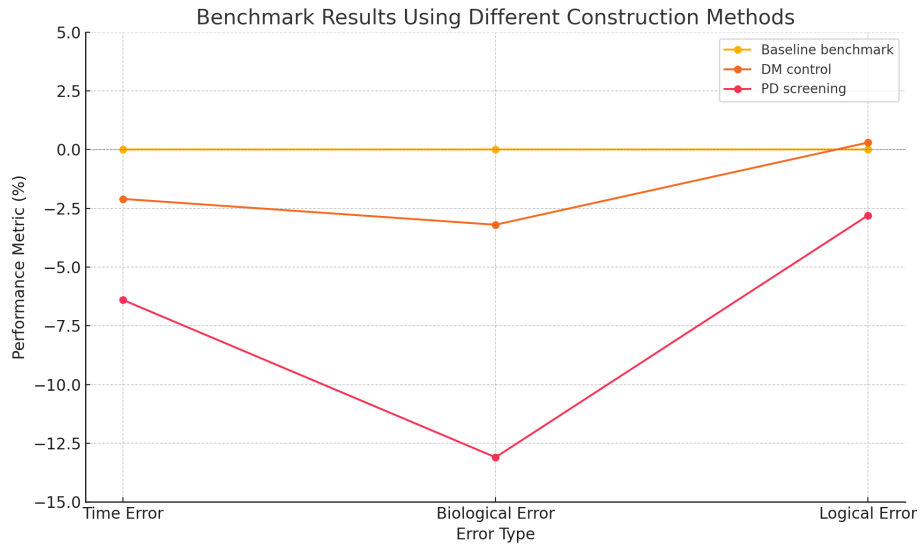

Fig. 6. Benchmark Results Using Different Construction Methods: Average performance metrics of four LVLMs across different error types (temporal, biological, logical) are compared using three different benchmarks. The yellow line represents the original synthetic benchmark, the orange line represents the human-authored prompts benchmark, and the red line represents the manually screened and labeled benchmark. LVLMs achieve similar results on yellow and orange lines

8   Conclusion

The exploration into the proficiency of Large Vision-Language Models (LVLMs) in discerning AI-generated images versus human-created ones has yielded illuminating insights. Our comprehensive study, juxtaposing LVLMs against human participants, reveals a pronounced disparity in their capabilities. Human participants demonstrated exceptional accuracy, significantly outperforming LVLMs, which exhibited inherent limitations in recognizing AI-generated imagery.

Based on these findings, we developed a new benchmark that leverages the unique ability of AI to generate hard-to-obtain images, and proposed a robust framework to evaluate the misidentification ability of LVLMs using synthetic data. This approach enhances the scalability and flexibility of the benchmark, and making it resistant to data contamination. This ensures that the models are rigorously tested on their true capabilities rather than their familiarity with training data.

This study delineates the current landscape of LVLM proficiency, demonstrating a novel approach for creating synthetic benchmarks on visio-linguistic abilities. It provides valuable experiments and data to support subsequent related research, paving the way for further advancements in the evaluation and development of LVLMs. Our findings underscore the necessity for continuous improvement in LVLMs to bridge the gap between human and machine capabilities in image recognition and understanding.

Limitations

While our methodology aims to leverage AI for generating a comprehensive and diverse set of benchmarks, inherent limitations exist in both text-to-image (T2I) models and large language models (LLMs). The T2I models sometimes struggle to produce erroneous images following specific instructions, and LLMs exhibit limited ability to understand this characteristic of T2I models and craft clear, precise instructions for T2I models. This can introduce noise into the synthetic data, leading to less pronounced or unobservable errors and weakening the accuracy of the benchmarks.

To address this issue, we plan to enhance the precision of generated data and further reduce noise. Our efforts include constructing more powerful LLM agents combined with state-of-the-art T2I models, which we believe will help alleviate these challenges. By improving the clarity and specificity of instructions given to T2I models, and by refining the error generation process, we aim to create benchmarks that are both highly accurate and representative of real-world complexities. This will ultimately strengthen the evaluation process and contribute to more robust and reliable performance assessments of LVLMs.

References

1. OpenAI. (n.d.). Dall-E 3. https://openai.com/index/dall-e-3/

2. Stability AI image models. Stability AI. (n.d.). https://stability.ai/stable-image
3. Midjourney. (n.d.). Midjourney. https://www.midjourney.com/
4. He, K., Zhang, X., Ren, S., & Sun, J. (2016). Deep residual learning for image recognition. 2016 IEEE Conference on Computer Vision and Pattern Recognition (CVPR). https://doi.org/10.1109/cvpr.2016.90
5. Touvron, H., Cord, M., Douze, M., Massa, F., Sablayrolles, A., & Jegou, H. (2021, July 1). Training data-efficient image transformers & distillation through attention. PMLR. https://proceedings.mlr.press/v139/touvron21a.html
6. Liu, Z., Lin, Y., Cao, Y., Hu, H., Wei, Y., Zhang, Z., Lin, S., & Guo, B. (2021). Swin Transformer: Hierarchical vision transformer using shifted windows. 2021 IEEE/CVF International Conference on Computer Vision (ICCV). https://doi.org/10.1109/iccv48922.2021.00986
7. Zhu, M., Chen, H., Yan, Q., Huang, X., Lin, G., Li, W., Tu, Z., Hu, H., Hu, J., & Wang, Y. (2023, June 24). Genimage: A million-scale benchmark for detecting AI-generated image. arXiv.org. https://arxiv.org/abs/2306.08571
8. Yu, W., Yang, Z., Li, L., Wang, J., Lin, K., Liu, Z., Wang, X., & Wang, L. (2023, October 24). MM-vet: Evaluating large multimodal models for integrated capabilities. arXiv.org. https://arxiv.org/abs/2308.02490
9. Guan, T., Liu, F., Wu, X., Xian, R., Li, Z., Liu, X., Wang, X., Chen, L., Huang, F., Yacoob, Y., Manocha, D., & Zhou, T. (2023, November 28). Hallusionbench: An advanced diagnostic suite for entangled language hallucination & visual illusion in large vision-language models. arXiv.org. https://arxiv.org/abs/2310.14566
10. Hessel, J., Marasović, A., Hwang, J. D., Lee, L., Da, J., Zellers, R., Mankoff, R., & Choi, Y. (2023, July 6). Do androids laugh at Electric Sheep? humor "understanding" benchmarks from the New Yorker Caption Contest. arXiv.org. https://arxiv.org/abs/2209.06293
11. Yue, X., Ni, Y., Zhang, K., Zheng, T., Liu, R., Zhang, G., Stevens, S., Jiang, D., Ren, W., Sun, Y., Wei, C., Yu, B., Yuan, R., Sun, R., Yin, M., Zheng, B., Yang, Z., Liu, Y., Huang, W., ... Chen, W. (2023, December 21). MMMU: A massive multi-discipline multimodal understanding and reasoning benchmark for expert AGI. arXiv.org. https://arxiv.org/abs/2311.16502
12. Bitton, Y., Bansal, H., Hessel, J., Shao, R., Zhu, W., Awadalla, A., Gardner, J., Taori, R., & Schmidt, L. (2023, December 26). VisIT-Bench: A benchmark for vision-language instruction following inspired by real-world use. arXiv.org. https://arxiv.org/abs/2308.06595
13. Bitton, Y., Yosef, R., Strugo, E., Shahaf, D., Schwartz, R., & Stanovsky, G. (2022, December 8). VASR: Visual analogies of situation recognition. arXiv.org. https://arxiv.org/abs/2212.04542
14. Saharia, C., Chan, W., Saxena, S., Li, L., Whang, J., Denton, E., Ghasemipour, S. K. S., Ayan, B. K., Mahdavi, S. S., Lopes, R. G., Salimans, T., Ho, J., Fleet, D. J., & Norouzi, M. (2022, May 23). Photorealistic text-to-image diffusion models with deep language understanding. arXiv.org. https://arxiv.org/abs/2205.11487
15. Feng, W., He, X., Fu, T.-J., Jampani, V., Akula, A., Narayana, P., Basu, S., Wang, X. E., & Wang, W. Y. (2023, February 28). Training-free structured diffusion guidance for compositional text-to-image synthesis. arXiv.org. https://arxiv.org/abs/2212.05032
16. Bordes, F., Shekhar, S., Ibrahim, M., Bouchacourt, D., Vincent, P., & Morcos, A. S. (2023, December 13). Pug: Photorealistic and semantically controllable synthetic data for representation learning. arXiv.org. https://arxiv.org/abs/2308.03977